Ground-State Kinetics of Bistable Redox-Active Donor−Acceptor Mechanically Interlocked Molecules

ALBERT C. FAHRENBACH,[†] CARSON J. BRUNS,[†] HAO LI,[†]
ALI TRABOLSI,[‡] ALI COSKUN,[§] AND J. FRASER STODDART[†,*]

[†]Department of Chemistry, Northwestern University, 2145 Sheridan Road, Evanston, Illinois 60208-3113, United States, [‡]Department of Chemistry, New York University, Abu Dhabi, United Arab Emirates, and [§]NanoCentury Institute and Graduate School of Energy, Environment, Water, and Sustainability (World Class University), Korea Advanced Institute of Science and Technology (KAIST) 373-1 Guseong Dong, Yuseong Gu, Daejeon 305-701, Republic of Korea

CONSPECTUS

The ability to design and confer control over the kinetics of the processes involved in the mechanisms of artificial molecular machines is at the heart of the challenge to create ones that can carry out useful work on their environment, just as Nature is wont to do. As one of the more promising forerunners of prototypical artificial molecular machines, chemists have developed bistable redox-active donor−acceptor mechanically interlocked molecules (MIMs) over the past couple of decades. These bistable MIMs generally come in the form of [2]rotaxanes, molecular compounds that constitute a ring mechanically interlocked around a dumbbell-shaped component, or [2]catenanes, which are composed of two mechanically interlocked rings. As a result of their interlocked nature, bistable MIMs possess the inherent propensity to express controllable intramolecular, large-amplitude, and reversible motions in response to redox stimuli. In this Account, we rationalize the kinetic behavior in the ground state for a large assortment of these types of bistable MIMs, including both rotaxanes and catenanes. These structures have proven useful in a variety of applications ranging from drug delivery to molecular electronic devices.

...Ground-State Kinetics...

k_f k_b

MSCC   GSCC

Bistable Redox-Active Donor-Acceptor MIMs

These bistable donor−acceptor MIMs can switch between two different isomeric states. The favored isomer, known as the ground-state co-conformation (GSCC) is in equilibrium with the less favored metastable state co-conformation (MSCC). The forward (k_f) and backward (k_b) rate constants associated with this ground-state equilibrium are intimately connected to each other through the ground-state distribution constant, K_{GS}. Knowing the rate constants that govern the kinetics and bring about the equilibration between the MSCC and GSCC, allows researchers to understand the operation of these bistable MIMs in a device setting and apply them toward the construction of artificial molecular machines.

The three biggest influences on the ground-state rate constants arise from (i) ground-state effects, the energy required to breakup the noncovalent bonding interactions that stabilize either the GSCC or MSCC, (ii) spacer effects, where the structures overcome additional barriers, either steric or electrostatic or both, en route from one co-conformation to the other, and (iii) the physical environment of the bistable MIMs. By managing all three of these effects, chemists can vary these rate constants over many orders of magnitude. We also discuss progress toward achieving mechanostereoselective motion, a key principle in the design and realization of artificial molecular machines capable of doing work at the molecular level, by the strategic implementation of free energy barriers to intramolecular motion.
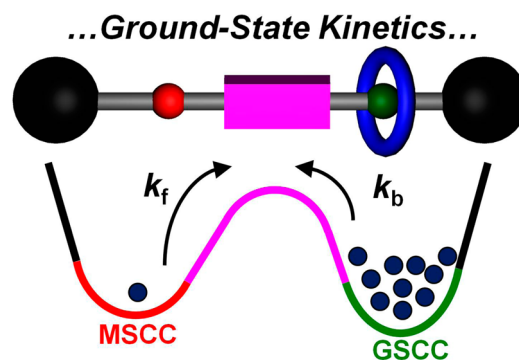
Introduction

The time scale on which human beings perceive natural events is a unique one. The random mutations that occur in our DNA that power evolution by means of natural selection may appear impossibly slow, while the molecular machines that support life ubiquitously across the plant and animal kingdoms may at times seem impossibly fast. It is essential that we understand the kinetics of

biological molecular machines, because their efficient operation by dint of complex mechanisms leads to the ability to support life as we know it on our planet. For example, the active transport protein bacteriorhodopsin[1] is a biological molecular machine that uses energy in the form of light to pump protons across the cell membrane against a concentration gradient, that is, away from equilibrium. It is widely accepted[2] that in order for molecular machines to do work on their molecular environment, for example, pushing a reaction uphill away from its equilibrium state, they must rely on a ratchet mechanism. A considerable amount of theoretical work has been carried out[3,4] toward investigating the possibilities of employing an assortment of different types of ratchet mechanisms. Despite the variety of proposed ratchet mechanisms that exist, an oft shared component of each depends on the ability of the experimentalist, by means of an applied stimulus, to raise and lower thermodynamic wells, while manipulating the energy barriers that border these wells, such that the reaction under consideration is liable to proceed along the most kinetically favored pathway and not necessarily the most favored thermodynamic one. As a consequence, in order to employ a ratchet mechanism in the design and synthesis of artificial molecular machines, a clear understanding of their operation, together with an ability to control the kinetic pathways involved in their mechanisms of switching, are requisite.

In the pursuit of artificial molecular machines possessing functions and operations that find their inspiration in nature, a vast number of molecular switches have emerged[4,5] as prototypes. Some of the most prominent examples are capable of demonstrating actuation on a macroscopic scale. Doubly bistable palindromic rotaxanes,[6] which can bend microcantilevers, rotary motors mounted on surfaces that can rotate[7] macroscopic objects, and liquid crystalline elastic polymers, capable of rotating[8] a set of pulleys upon exposure to light, have all been demonstrated. The design and synthesis of molecular machines capable of doing work at the *molecular* scale, however, have been few and far between.

Molecular switches in the form of bistable redox-active donor−acceptor mechanically interlocked molecules[9] (MIMs) are a type of switch (Figure 1A) capable of undergoing large amplitude and controllable relative intramolecular motion. A firm mechanistic understanding of the kinetics of their switching behavior has been crucial in the development of their potential applications in the context of artificial molecular actuators[10] and muscles,[11] nanovalves[12] for drug delivery vehicles, and molecular memory[13] devices. In the case of molecular electronic devices, which employ these
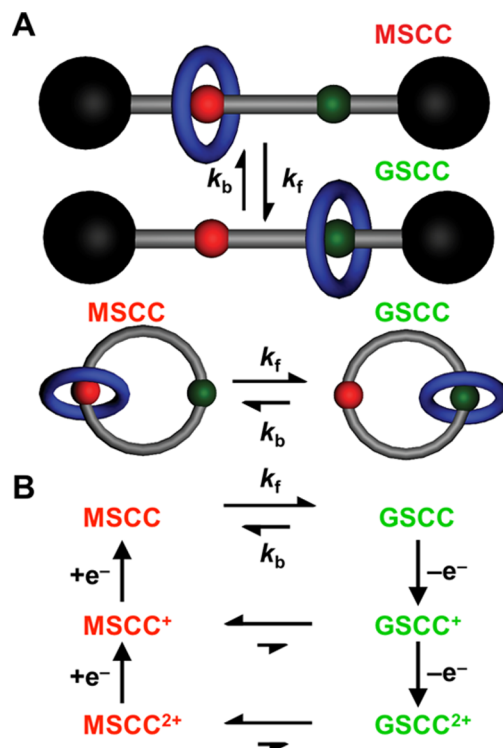
FIGURE 1. (A) Generalized graphical representations of a bistable [2]rotaxane (top) and a bistable [2]catenane (bottom) undergoing relative translational or circumrotational movements, so as to interconvert these MIMs between their ground-state co-conformation (GSCC) and metastable-state co-conformation (MSCC) at rates determined by the rate constants k_f and k_b. (B) Electrochemical mechanism of switching of a bistable MIM, which results in overpopulation of the MSCC that persists for some time before relaxing back to the GSCC by an amount dictated by the ground-state distribution constant $K_{GS} = k_f/k_b$. Note that switching can also occur by reduction in some cases.

bistable MIMs as their active binary components, the kinetics governing their ground-state shuttling behavior is proposed to be directly linked to the volatility of the device. In order for MIMs to serve as molecular machines that can do work at the molecular level by means of a ratchet mechanism, control over the kinetics of their relative motions is crucial. In this Account, we analyze our research over the past couple of decades on the ground-state kinetics of redox-active bistable donor−acceptor MIMs.

Mechanism of Switching: The Metastable State

A similar electrochemical mechanism of switching (Figure 1B) is shared by all the bistable MIMs discussed in this Account. In the ground state, these MIMs[14] exist as a thermodynamic distribution between two co-conformations at equilibrium. The more stable one is given the name ground-state co-conformation (GSCC), while the less stable one is called the metastable-state co-conformation (MSCC).

The distribution of MSCC to GSCC is characterized by a unitless equilibrium constant:

$$[MSCC] \overset{K_{GS}}{\rightleftharpoons} [GSCC]$$

where K_{GS} is the ground-state distribution constant. The kinetics associated with this equilibrium can be expressed as:

$$[MSCC] \underset{k_b}{\overset{k_f}{\rightleftharpoons}} [GSCC]$$

where k_f is the rate of the forward co-conformational isomerism, leading to the GSCC, and k_b is the rate of the backward co-conformational isomerism leading, to the MSCC. From these two equations, the following relationship is apparent:

$$K_{GS} = \frac{k_f}{k_b}$$

In the case of these bistable MIMs, oxidation or reduction of the unit encircled by a ring in the GSCC results in a loss of affinity by the ring and is caused typically by the disruption of the donor—acceptor interactions and Coulombic repulsions or both. This loss of affinity leads to a shift in the co-conformational distribution toward the unit associated with the MSCC. Return of the unit back to its original oxidation state results in a scenario where the MSCC is populated to an extent that is higher than that found under equilibrium conditions. Consequently, the concentration of the MSCC begins to decrease as it is converted more and more into the GSCC at a rate proportional to k_f until equilibrium is attained. Under the appropriate experimental conditions, it is possible to detect the change in concentration of the MSCC as a function of time. For a detailed mathematical consideration of the kinetics of this mechanistic model, see ref 31.

The importance of the role played by the ground-state kinetics in these bistable MIMs first became clear to us in the context of molecular memory devices, which employ these MIMs as the active binary components. In 2000, we reported[15] on the fabrication of a molecular memory device that utilizes (Figure 2) the bistable [2]catenane **C1**[4+] sandwiched between top and bottom electrodes in a molecular switch tunnel junction (MSTJ). The structure of these [2]catenane molecules consists of a π-electron-poor cyclobis(paraquat-*p*-phenylene)[16] (CBPQT[4+]) ring mechanically interlocked with a macrocyclic polyether incorporating a redox-active tetra-thiafulvalene (TTF) along with a 1,5-dioxynaphthalene (DNP) π-electron-rich unit. The GSCC for this bistable catenane is
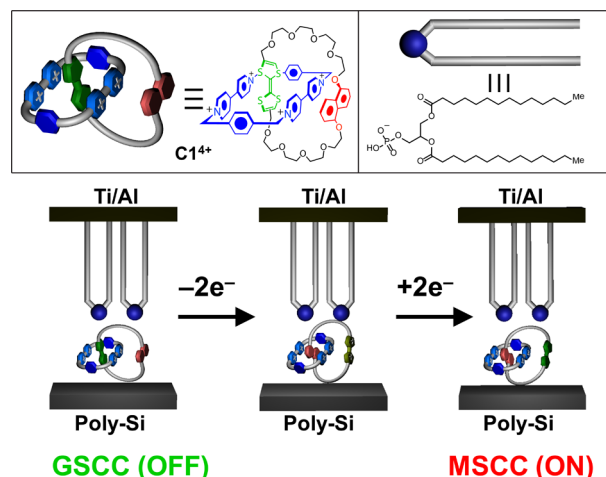

FIGURE 2. Schematic representation of the switching process of a bistable [2]catenane **C1**[4+], which occurs in the context of a molecular switch tunnel junction (MSTJ). The MSCC represents the switch-closed "ON" state and the GSCC the switch "OFF" state.

defined when the CBPQT[4+] ring encircles the TTF unit, and the MSCC is defined when the ring encircles the DNP unit. The ground-state distribution constant K_{GS} favors[17] the GSCC over the MSCC by a ratio of approximately 150:1, at least in MeCN solution. The need to explain this device behavior resulted in our postulating that after an oxidation/reduction cycle of the TTF unit, the MSCC, which has the CBPQT[4+] ring encircled around the DNP unit, is trapped kinetically. The existence of the MSCC is crucial in the design of molecular electronic devices that employ these bistable MIMs as the active binary components and has been a prime motivator for conducting further investigations[18] of the ground-state kinetics in these bistable MIMs.

Kinetics across Different Environments

Although the existence of the metastable state was a crucial element in explaining the mechanism of operation of molecular memory devices based on MSTJs, little in the way of direct observation of this co-conformation was at hand initially. The situation, however, changed in 2004. Around this time, we began[19] a systematic electrochemical investigation employing variable scan-rate, variable temperature cyclic voltammetry (CV) to determine the role of physical environment on the ground-state kinetics in a series of bistable redox-active MIMs with the focus on the lifetimes of the metastable states. The bistable MIMs included both [2]rotaxanes and [2]catenanes, each one incorporating TTF and DNP units in its polyether dumbbell or ring component, mechanically interlocked with either the CBPQT[4+] or cyclo-bis(diazapyrenium-*p*-phenylene)[20] (CBDAP[4+]) ring. In order
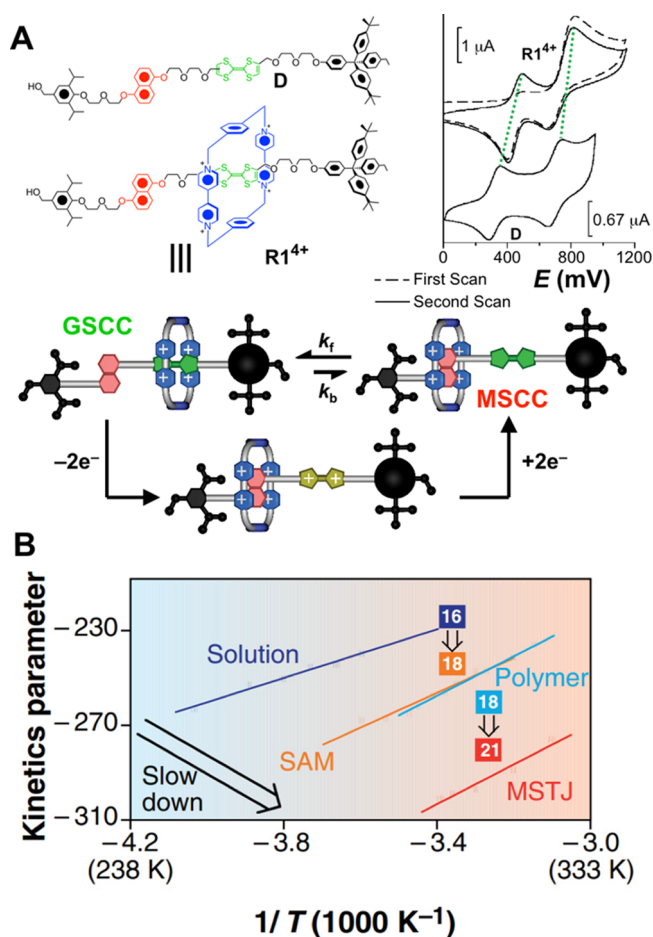
FIGURE 3. (A) The structural formula of the bistable [2]rotaxane $R1^{4+}$ and the dumbbell **D**, the graphical representation of $R1^{4+}$, and its simplified electrochemical mechanisms of switching. In the upper right is the CV of the [2]rotaxane (top) along with its free dumbbell (bottom). CV Data from ref 19. Reprinted with permission from John Wiley and Sons. (B) Plot of the kinetic data for the [2]rotaxane, illustrating that the free energy barrier $\Delta G^{\ddagger}(k_f)$ for relaxation of the MSCC increases from 16 to 21 kcal mol^{-1} upon changing physical environments from solution to SAMs to a polymer matrix to MSTJs. Figure from ref 21. Reprinted with permission from AAAS.

to provide a representative example[19] of the data obtained from variable scan-rate CV experiments and its mechanistic interpretation, consider (Figure 3A) the case of the bistable [2]rotaxane $R1^{4+}$ composed of the CBPQT^{4+} ring mechanically interlocked around a dumbbell containing TTF and DNP units. Quantification of the first oxidation wave arising from the TTF unit in the second scan at different scan rates provides a measure of the amount of MSCC present as a function of time following an oxidation/reduction cycle of the TTF unit from which the forward rate constant k_f can be extracted. Using this methodology, the ground-state kinetics of a series of bistable MIMs were investigated across different physical environments.

As a trend, the relaxation rate constant k_f of the metastable state of $R1^{4+}$ was observed[19,21] (Figure 3B) to decrease by over an order of magnitude as the MIMs were transferred from MeCN solution ($\Delta G^{\ddagger}(k_f) = \sim16$ kcal mol^{-1}) to a more viscous polymer matrix ($\Delta G^{\ddagger}(k_f) = \sim18$ kcal mol^{-1}). A self-assembled monolayer (SAM)[22] on gold surfaces of bistable [2]rotaxanes similar in structure to $R1^{4+}$ but with a disulfide tether on one end of the dumbbell was also investigated. The relaxation of the MSCC was observed to be slowed by about the same amount on moving from MeCN solution to the SAM, a situation that can be considered as a "half-device" in relation to a MSTJ. Transferring the bistable rotaxane from the SAM to a MSTJ led to a decrease in the rate constant k_f by about another 100-fold ($\Delta G^{\ddagger}(k_f) = 21$ kcal mol^{-1}). These examples show that the kinetics of the ground-state shuttling processes depend heavily on their surrounding environment.

Ground-State and Spacer Effects

The free energy barrier governing the circumrotational or translational motion in a bistable MIM can typically be divided (Figure 4) into two components. The first component is a result of what we refer to here as ground-state effects, a concept that can be thought of as the energy necessary to break the noncovalent bonding interactions that serve to stabilize either the GSCC or the MSCC. Usually, these interactions involve[9] (i) face-to-face donor−acceptor stacking between π-electron-rich and π-electron-poor units, (ii) [C−H···O] hydrogen bonding from polyether oxygens and protons on electropositive carbons, and, in the context of water, (iii) hydrophobic interactions. In the case of bistable rotaxanes, side-on π−π donor−acceptor interactions, which
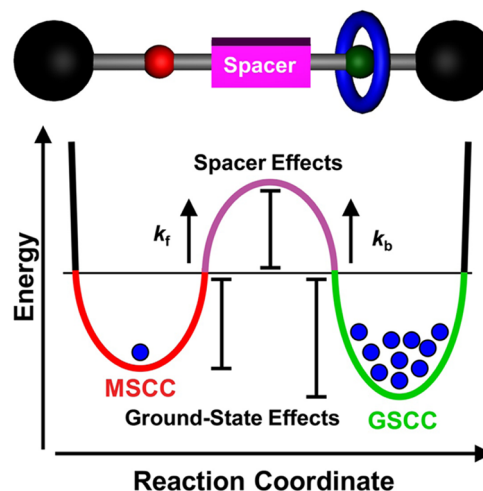
FIGURE 4. Reaction coordinate profile illustrating the difference between ground-state and spacer contributions to the free energy of activation needed to undergo translation.

usually occur when the secondary donor (or acceptor) unit on the thread portion of the dumbbell stacks alongside the outside of the ring, may lead[23] to modest contributions to the ground-state energy worth around 0.5 kcal mol^{-1}. In some bistable catenanes, this same type of alongside $\pi-\pi$ donor−acceptor interaction is enforced[17] by the geometric constraints of the structure, leading to significantly greater contributions to the ground-state energy. The second component of the free energy barrier consists of the energy required to translate the ring across the spacer unit that connects the two different π-electron units in the ring or dumbbell component together: we refer to this component as the spacer effect.

In order to illustrate an example of the ground-state effect in action, consider the following series (Figure 5) of three bistable [2]catenanes: one **C2**$^{4+}$, composed[24] of a crown ether incorporating TTF and a dialkyne unit, mechanically interlocked with the CBPQT^{4+} ring; another **C1**$^{4+}$, consisting[25] of a crown ether with TTF and DNP units; and a third[19] **C3**$^{4+}$ containing the same crown ether but involving a CBDAP^{4+} ring. In the case of the first [2]catenane, **C2**$^{4+}$, the MSCC, which has the CBPQT^{4+} ring positioned over the dialkyne unit, is so unstable compared with the GSCC that the rate of relaxation is too fast to be measured ($\Delta G^{\ddagger}(k_f) < 14.8$ kcal mol^{-1}). This rapid relaxation is a consequence of the fact that the $\pi-\pi$ donor−acceptor interactions between the dialkyne unit and the CBPQT^{4+} ring are extremely weak, most likely as a result[17] of the
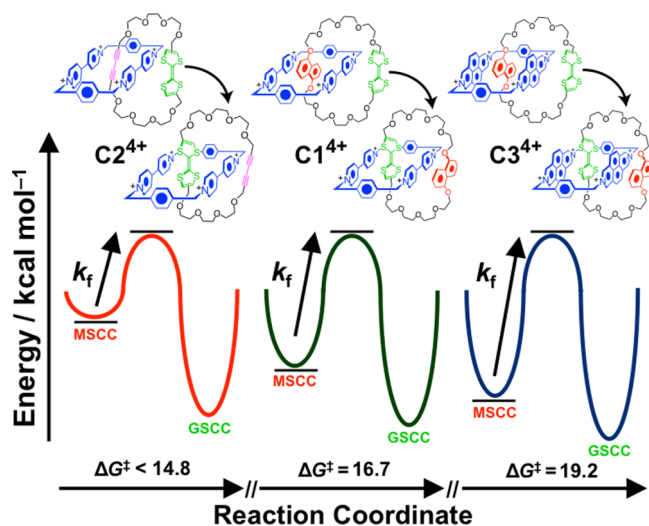
FIGURE 5. Reaction coordinate profile for a series of three bistable redox-active bistable [2]catenanes, **C2**$^{4+}$, **C1**$^{4+}$, and **C3**$^{4+}$, in their ground states. In each case, although contributions to the free energy barrier for conversion of the MSCC to the GSCC from spacer effects are the same, contributions from ground-state effects increase the activation free energy barrier across the series.

TABLE 1. Rate Constants and Free Energy Barriers for the Ground-State Circumrotation of Some Bistable Donor−acceptor Catenanes under Various Conditions[e]

Environment	T (K)	$\Delta G_f^{\ddagger}$ (k_f) kcal·mol^{-1} (s^{-1})	$\Delta G_b^{\ddagger}$ (k_b) kcal·mol^{-1} (s^{-1})	Ref
C2^{4+}				
CH$_3$CN[a]	298	4.2 (5.1×10^9)[b]	9.7 (4.5×10^5)[c]	24
C1^{4+}				
CH$_3$CN[a]	283	16.1 (2.1)	-	19
CH$_3$CN[a]	298	16.7 (4.1)	20.3 (8.0×10^{-3})[c]	19
Polymer	298	17.0 (1.6)	-	19
C3^{4+}				
CH$_3$CN[a]	298	19.2 (5.7×10^{-2})	-	19
Polymer	298	21.0 (1.3×10^{-3})	-	19
H$_2$O:CH$_3$CN (1:1)	298	14.1 (300)	16.1 (10)	28
H$_2$O[d]	298	17.5 (1.21)	-	27
CD$_3$CN	343	28.5 (4.8×10^{-6})	28.8 (3.2×10^{-6})	26

^{a}With 0.1 M NBu$_4$PF$_6$. ^{b}Estimated using computational models. ^{c}Calculated from K_{GS}, see ref 14. ^{d}With 0.1 M NBu$_4$Cl. $^e\Delta G^{\ddagger}$ free energy barriers were calculated by means of the Eyring equation.

HOMO−LUMO energy mismatch, so only a small amount of energy is required to break up these noncovalent bonding interactions, allowing circumrotation by the crown ether to occur. In comparison with the second [2]catenane, **C1**$^{4+}$, the π-donor−acceptor interactions of the DNP unit with the CBPQT^{4+} ring in the MSCC are very much stronger compared with those involving the dialkyne, so the energy required for the crown ether to undergo circumrotation is substantially larger. The free energy barrier to circumrotation $\Delta G^{\ddagger}(k_f)$ is 16.7 kcal mol^{-1}. In the case of the third [2]catenane, **C3**$^{4+}$, the donor−acceptor interactions between the DNP unit and the CBDAP^{4+} ring are even greater, so the free energy barrier $\Delta G^{\ddagger}(k_f)$ to circumrotation by the crown ether is raised to 19.2 kcal mol^{-1}. For additional comparisons of free energy barriers in bistable catenanes and rotaxanes, see Tables 1[19,24,26−28] and 2.[19,29−33]

TABLE 2. Rate Constants and Free Energy Barriers for the Ground-State Translation of Some Bistable Donor−acceptor Rotaxanes under Various Conditions[d]

Rotaxane	Environment	T (K)	$\Delta G_f^{\ddagger}$ (k_f) kcal·mol⁻¹ (s⁻¹)	$\Delta G_b^{\ddagger}$ (k_b) kcal·mol⁻¹(s⁻¹)	Ref
	CH_3CN[a]	298	17.7 (6.9×10⁻¹)	18.3 (0.23)[b]	31
	Polymer	298	19.2 (5.9×10⁻²)	-	31
	MSJT	298	21.7 (8.4×10⁻⁴)	-	31
	CH_3CN[a]	278	15.9 (1.8)	-	19
	CH_3CN[a]	298	16.2 (8.1)	17.5 (0.90)[b]	19
	Polymer	298	18.1 (0.29)	-	19
	SAM	278-303	17.7[c] (-)	-	19
	CD_3COCD_3	300	24 (2×10⁻⁵)	24 (2×10⁻⁵)[b]	29
	CD_3SOCD_3	300	22 (3×10⁻⁴)	22 (3×10⁻⁴)[b]	29
	CD_3COCD_3	293	14.8 (60)	15.6 (15)[b]	30
	CD_3CN	298	23.5 (3.3×10⁻⁵)[b]	23.8 (2.2×10⁻⁵)	33
	CH_3CN[a]	298	19 (4×10⁻²)	21 (4×10⁻³)[b]	32

[a]With 0.1 M NBu_4PF_6. [b]Calculated from K_{GS}. [c]E_A averaged over the specified range of T. [d]$\Delta G^{\ddagger}$ free energy barriers were calculated by means of the Eyring equation, unless otherwise noted.

Steric Spacers

Steric spacers can serve to slow the rate of circumrotation or shuttling significantly in bistable MIMs. We have more deliberately sought to investigate, in a systematic fashion, the effect of steric spacers placed between the two π-electronic units on the translational motion in bistable [2]rotaxanes. Resorting to employing degenerate systems in place of bistable ones as models simplifies both the synthesis and physical characterization. In one particular investigation, we have examined[34] (Figure 6A) the effect that a series of three differently sized spacers located between the DNP units has upon the shuttling of the CBPQT[4+] ring. The three spacers examined were tetra(ethylene glycol) (**R2**[4+]), terphenylene (**R3**[4+]), and diphenyl ether (**R4**[4+]), and perhaps somewhat unexpectedly, although the free energy barriers, $\Delta G^{\ddagger}$, to shuttling are nearly the same in each case, their activation parameters, $\Delta H^{\ddagger}$ and $\Delta S^{\ddagger}$, revealed significant differences. The rotaxane with the smallest enthalpy of activation ($\Delta H^{\ddagger} = 12.7$ kcal mol⁻¹) is the one (**R2**[4+]) with the tetra(ethylene glycol) spacer, but it also has the highest entropic penalty ($\Delta S^{\ddagger} = -9.3$ cal mol⁻¹ K⁻¹). The rotaxane **R4**[4+] with the diphenyl ether has the highest enthalpic penalty ($\Delta H^{\ddagger} = 14.5$ kcal mol⁻¹) yet has the smallest entropic one ($\Delta S^{\ddagger} = -3.2$ cal mol⁻¹ K⁻¹). The rotaxane **R3**[4+] with the terphenylene spacer occupies the middle ground ($\Delta H^{\ddagger} = 13.6$ kcal mol⁻¹; $\Delta S^{\ddagger} = -4.8$ cal mol⁻¹ K⁻¹). This investigation has alerted us to the need to consider carefully (i) enthalpic effects, emanating from steric bulk, and (ii) increases in entropy, which take place at the transition state, when introducing steric spacers into bistable MIMs. For additional comparisons of the effects of different steric spacers on the free energy barriers in degenerate rotaxanes, see Table 3.[35−44]

The ability to modulate the kinetics between fast and slow rates in a reversible manner in a bistable MIM may have fundamental consequences for the construction of artificial molecular machines whose operations depend on employing a ratchet mechanism. In pursuit of this goal, we designed and synthesized[45] (Figure 6B) a bistable [2]rotaxane, **R5**[4+], incorporating TTF and DNP units flanking a central tetramethylazobenzene steric spacer. When the azobenzene unit adopts the *trans* configuration, the CBPQT[4+] ring, which is mechanically interlocked around the dumbbell component, experiences a smaller free energy barrier ($\Delta G^{\ddagger}$) to shuttling than when the azobenzene unit is in the *cis* configuration. The rate limiting step to recovery of the GSCC is not the shuttling of the ring over the *cis*-azobenzene unit but rather the thermal isomerization of the azobenzene
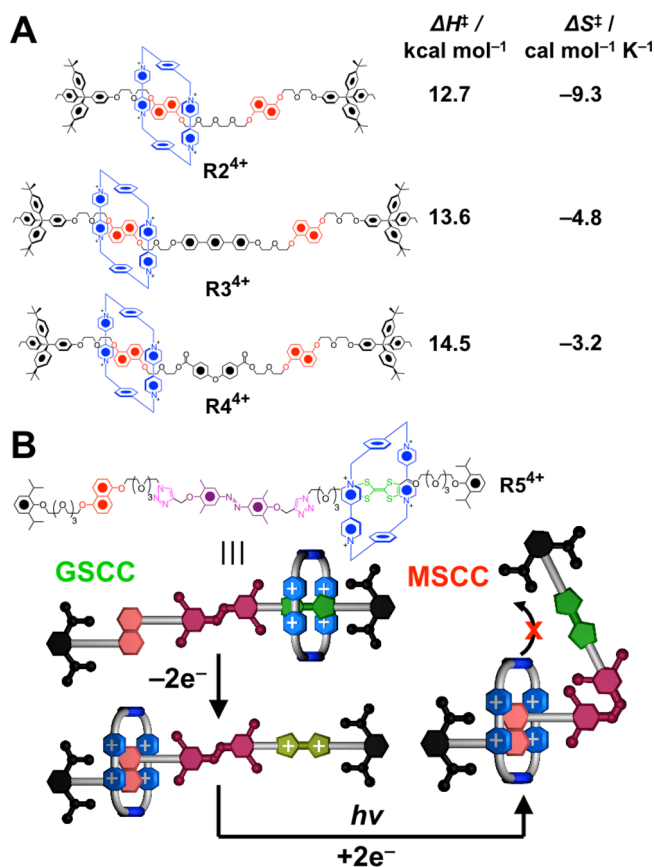
FIGURE 6. (A) A series of three degenerate [2]rotaxanes, $R2^{4+}$, $R3^{4+}$, and $R4^{4+}$, with different spacers connecting two DNP units and the kinetic parameters characterizing the translational motion of the ring. (B) A bistable [2]rotaxane $R5^{4+}$ incorporating a tetramethylazobenzene spacer. In the *cis* form, the azobenzene acts as a steric barrier, which effectively prohibits relaxation of the MSCC following an oxidation/reduction cycle carried out on the TTF unit.

unit back to its *trans* configuration. By *trans*-to-*cis* isomerization of the azobenzene after oxidation of the TTF unit, relaxation of the MSCC, following reduction of the TTF back to its neutral form, can be stopped altogether.

Electrostatic Spacers

We later became interested in studying the effect that electrostatic spacers have on the ground-state kinetics in bistable MIMs, in the case where a charged ring component is present. Some of our first investigations involved[46,47] examining a variety of different positively charged spacers incorporated between two DNP units in a series of degenerate [2]rotaxanes. One of these charged spacers included[47] (Figure 7A) a bipyridinium dication ($BIPY^{2+}$) in $R6^{6+}$. The rate of shuttling of the $CBPQT^{4+}$ ring in this degenerate [2]rotaxane was slowed to such an extent that we were unable to measure the rate by dynamic ^1H NMR spectroscopy, indicating the free energy barrier to be greater than
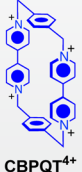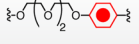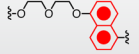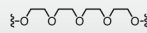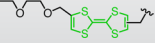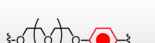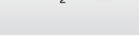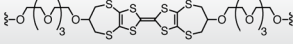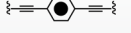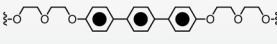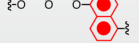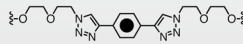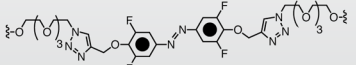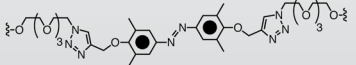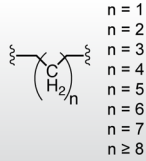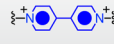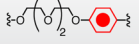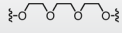
17 kcal mol^{-1} (D$_2$O, 343 K). In order to gain additional insight into the heights of these electrostatic barriers, we performed[47] an investigation on the kinetics of a host—guest complex (Figure 7B) in which the host is the $CBPQT^{4+}$ ring and the guest is a DNP unit flanked on each side by covalently attached $BIPY^{2+}$ electrostatic barriers. The unimolecular rate of dethreading of the [2]pseudorotaxane was on the order of 10^{-7} s^{-1} in 0.1 M NaCl in H$_2$O. In the knowledge that electrostatic units have a marked effect on the rate of threading and shuttling, next we incorporated[32] a $BIPY^{2+}$ unit into a bistable [2]rotaxane $R7^{6+}$ (Figure 7C) containing DNP and TTF units and investigated the effect it had on relaxation of the MSCC following an oxidation/reduction cycle of the TTF. The rate of relaxation k_f of the MSCC is slowed ($\Delta G^{\ddagger}(k_f) = 19$ kcal mol^{-1}) approximately 100-fold compared with the analogous bistable [2]rotaxane without a $BIPY^{2+}$ electrostatic barrier ($\Delta G^{\ddagger}(k_f) = 16$ kcal mol^{-1}).

Following these initial studies on degenerate [2]rotaxanes with electrostatic spacers, we decided to construct a series of [2]rotaxanes composed of $CBPQT^{4+}$ rings mechanically interlocked around dumbbells incorporating only a central $BIPY^{2+}$ unit flanked on either side by oligomethylene chains (Table 3, row 4) of varying lengths. These rotaxanes devoid of any π-electron donors were synthesized[44] using a threading-followed-by-stoppering template-directed protocol reliant on radical—radical interactions. Presumably, since the $CBPQT^{4+}$ rings encircle the oligomethylene chains as a result of Coulombic repulsion from the $BIPY^{2+}$ unit and do not experience any stabilizing noncovalent bonding inte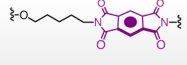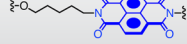ractions, the free energy barrier to shuttling of the rings is purely a result of the electrostatic spacer with no contributions from ground-state effects. As the oligomethylene chains of the dumbbells grow shorter, the free energy barrier to shuttling of the $CBPQT^{4+}$ rings over the central $BIPY^{2+}$ becomes less. This observation can be explained by the fact that the mechanical bond acts to force the $CBPQT^{4+}$ rings closer to the central $BIPY^{2+}$ unit at shorter chain lengths, which decreases the amount of thermal energy needed from the environment to clear the free energy barrier to shuttling, despite raising the repulsive Coulombic energy. In fact, the Coulombic repulsion energy becomes so large in the case of the [2]rotaxane with a dumbbell containing only three methylenes on each side of the central $BIPY^{2+}$, that the one-electron reduced radical product becomes stable under ambient conditions in an effort to minimize charge—charge repulsion!

Mechanostereoselectivity

In a recent publication, we introduced the term mechanostereochemical selectivity,[18] or mechanostereoselectivity,

TABLE 3. Rate Constants and Free Energy Barriers to Shuttling in Some Degenerate Donor—Acceptor Rotaxanes under Various Conditions[b]

Ring	Recognition Site	Spacer	Solvent	T K	ΔG‡ (k) kcal·mol⁻¹ (s⁻¹)	Ref
CBPQT⁴⁺			CD_3COCD_3	307	13.2 (2360)	35
			CD_3COCD_3 CD_3COCD_3	247 293	15.2 (0.2) 15.4 (20)	34
			CD_3COCD_3	293	17.5 (0.53)	34
			$(CD_3)_2NCHO$ CD_3SOCD_3 CD_3CN CD_3COCD_3	278 338 265 274	13.9 (71) 16.8 (98) 12.7 (169) 13.1 (187)	37
			CD_3COCD_3	208	10.3 (131)	42
			CD_3COCD_3	208	10.0 (119)	42
			CD_3COCD_3 CD_3COCD_3	236 293	14.8 (0.1) 15.1 (33)	34
			CD_3COCD_3 CD_3COCD_3	248 293	15.3 (0.2) 15.5 (19)	34
			CD_3COCD_3	296	15.5 (22)	41
			CD_3CN	322	15.6 (22)	43
			CD_3CN	350	>18 (<40)	43
	n = 1 n = 2 n = 3 n = 4 n = 5 n = 6 n = 7 n ≥ 8		CD_3COCD_3	238-251 256-267 256-258 266-271 287-303 300-321 295-29 330	11.4[a] (-) 12.3[a] (-) 12.7[a] (-) 13.7[a] (-) 14.6[a] (-) 15.4[a] (-) 15.8[a] (-) >16[a] (-)	44
			CD_3CN	350	18.1 (30)	38
HQ34C10			CD_3COCD_3	215	9.9 (338)	36
		R = Me Et Ph iPr tBu	CD_3CN	240 238 283 283 353	11.5 (157) 12.1 (38) 14.9 (20) 14.5 (38) >17.2 (<65)	39
DN38C10			CD_2Cl_2 CD_2Cl_2	226 294	11.4 (45) 10.9 (50k)	40
			CD_2Cl_2 CD_2Cl_2	266 294	14.1 (16) 14.0 (250)	40

[a] E_A averaged over the specified range of T. [b] ΔG‡ free energy barriers were calculated by means of the Eyring equation, unless otherwise noted.

to describe, in the case of MIMs or host—guest complexes, translational or circumrotational motions that happen faster kinetically along one path than another. To be sure, mechanostereoselective motion can only be obtained in
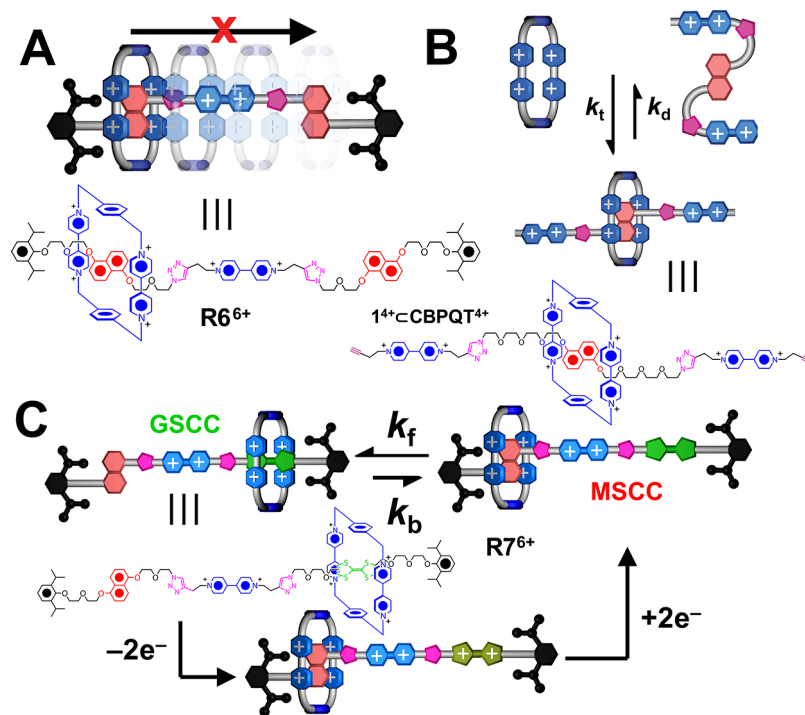
FIGURE 7. (A) A degenerate [2]rotaxane **R6**$^{6+}$ with a BIPY^{2+} spacer incorporated between two DNP units. The BIPY^{2+} unit increases the barrier to shuttling of the CBPQT^{4+} ring on account of Coulombic repulsions to such a degree that it was not able to be quantified by dynamic ^{1}H NMR spectroscopy. (B) The monomolecular dethreading rate constant for the complex 1^{4+} CCBPQT^{4+} is 5×10^{-7} s^{-1}, a value that corresponds to a free energy barrier of 26 kcal mol^{-1}. (C) The switchable [2]rotaxane **R7**$^{6+}$, which incorporates a BIPY^{2+} unit in between TTF and DNP units. The free energy barrier to relaxation of the MSCC to the GSCC following an oxidation/reduction cycle carried out on the TTF unit is 3 kcal mol^{-1} larger than that of the analgous [2]rotaxane lacking the central BIPY^{2+} spacer.

nondegenerate systems where the free energy barrier to the relative movement of the ring is smaller along one direction than it is along the other (Figure 8A), regardless of which path actually leads to the more thermodynamically stable state. In this manner, MIMs and host–guest systems can be made, in principle at least, to move away from their equilibrium distribution of co-conformations.

We have witnessed an example[18] (Figure 8B) of mechanostereoselectivity in the case of the [2]rotaxane **R7**$^{6+}$ incorporating BIPY^{2+}, TTF, and DNP units in its dumbbell component mechanically interlocked with the CBPQT^{4+} ring. The mechanism of switching for this multistable rotaxane was studied by variable scan rate CV. Upon reduction of the BIPY^{2+} units in both the ring and dumbbell components to their radical cationic state forming the trisradical **R7**$^{3(\bullet+)}$, the diradical dication CBPQT$^{2(\bullet+)}$ ring moves onto the BIPY$^{\bullet+}$ unit of the dumbbell as a consequence[18] of favorable radical–radical interactions. During reoxidation of **R7**$^{3(\bullet+)}$, a one-electron oxidation of the BIPY$^{\bullet+}$ radical of the CBPQT$^{2(\bullet+)}$ ring, which is not spin-paired with that of the dumbbell, occurs first. The resulting CBPQT$^{(2+)(\bullet+)}$ monoradical trication ring is capable of π-electronic donor–acceptor recognition and

so begins to undergo translation. The CBPQT$^{(2+)(\bullet+)}$ ring is confronted with two choices—it can shuttle toward either the DNP or the TTF unit. We found experimentally that the barrier to shuttling of the CBPQT$^{(2+)(\bullet+)}$ ring toward the TTF unit is lower by about 1.9 kcal mol^{-1} compared with the barrier for that toward the DNP unit. We speculate that self-folding of the TTF unit onto the BIPY^{2+} unit of the ring served to stabilize the transition state for shuttling along the TTF pathway. This lower barrier results in the mechanostereoselective translational motion. Another possible mechanism, which is consistent with the experimental data, is one in which the free energy barriers for translation of the ring toward DNP or TTF are the same, while the barrier for back translation onto the BIPY$^{\bullet+}$ radical cation is larger by 1.9 kcal mol^{-1} for TTF as a consequence of ground-state effects, a process for which the kinetics happen on the time scale of the CV experiment. This mechanism is not one which occurs by mechanostereoselectivity; rather the TTF unit is simply the more thermodynamically stable site for the ring to occupy. Unequivocal examples[48] of nontrivial mechanostereoselective motion in MIMs are few and far between and represent a major challenge in the field.
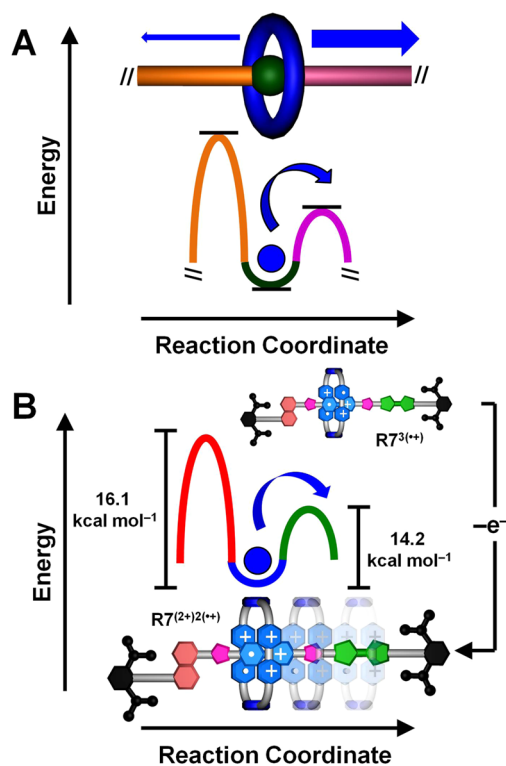
FIGURE 8. (A) Reaction coordinate profile illustrating the generalized concept of mechanostereoselective motion in the context of a MIM. (B) An example of mechanstereoselective motion in a [2]rotaxane (for the structural formula, see Figure 7B). Translation of the CBPQT$^{(2+)(\bullet+)}$ ring occurs faster onto the TTF unit as a consequence of a smaller free energy barrier.

Reflections

As our understanding of the kinetic behavior of bistable donor−acceptor MIMs has progressed, so too have the creative ways of controlling this behavior been expressed synthetically through design or physically by means of the environment in which they reside. Whether by use of steric or electrostatic spacers in the transition state or through the rational design of stabilizing noncovalent bonding interactions present in the ground state, the kinetics of bistable MIMs can be tuned precisely. The use of sophisticated spacers, which themselves can be switched between multiple states, is likely to lead to complex switching kinetics that will challenge our ability to be predictive of their behavior. Nonetheless, the road toward greater sophistication is exactly the one that needs to be taken in order to move beyond the realm of simple switches into the real world of molecular machines capable of performing meaningful work. As a means of increasing this sophistication, the concept of mechanostereoselectivity has significant practical importance when it comes to designing systems that operate by a ratchet mechanism. As a crucial ingredient to

their proposed operations, ratchet mechanisms depend on the ability of the experimentalist to employ precisely the type of mechanistic reaction pathways that lead to mechanostereoselective motion in the context of MIMs, wherein the energy barrier along one path is smaller than that along the other. By making use of both electrostatic and steric barriers, as well as molecular recognition processes that can be toggled using redox chemistry, we envision that mechanically interlocked molecular machines will be able to drive a system thermodynamically uphill by appropriately coupling it to the directed motion brought about by the ratchet mechanism of a mechanostereoselective actuation process. The general principles governing the kinetics of bistable donor−acceptor MIMs described in this Account will inform the development of sophisticated molecular machines that do genuine work, and we trust that we are one step more advanced along this path to molecular machines.

BIOGRAPHICAL INFORMATION

Albert C. Fahrenbach received an Honors B.Sc. Degree from Indiana University in 2008 in Chemistry, while conducting chemical synthesis under the tutelage of Professor Amar Flood. Albert received his Ph.D. Degree in organic chemistry with Professor Fraser Stoddart in 2013 at Northwestern University, (NU), where he focused on the design and synthesis of molecular switches and machines. Presently, he is a postdoctoral researcher in the group of Professor Jack Szostak in the Department of Chemistry and Chemical Biology at Harvard University.

Carson J. Bruns attended Luther College in Decorah, Iowa, with concentrations in chemistry and religion. After receiving his B.A. in Spring 2008, he joined the Stoddart and Stupp groups at NU to investigate the self-assembly of exotic interlocked architectures for his Ph.D. degree.

Hao Li received his B.Sc. and M.Sc. in Chemistry from Wuhan University, China. He performed his Ph.D. research under the supervision of Sir Fraser Stoddart at NU and is presently a postdoctoral fellow in the laboratory of Professor Jonathan Sessler at the University of Texas at Austin.

Ali Trabolsi during his Ph.D. at the University of Strasbourg studied supramolecular systems based on porphyrins, fullerenes, and oligo(phenylene vinylene). Formerly, Dr Trabolsi joined Sir Fraser Stoddart's group at the University of California, Los Angeles, as a research scholar and then at NU, where he focused on the synthesis and the characterization of mechanically interlocked molecules. He is now an assistant professor at New York University, Abu Dhabi.

Ali Coskun received all (B.Sc., M.Sc., Ph.D.) of his degrees in Chemistry from the Middle East Technical University, Turkey, while

carrying out his research activities under the supervision of Professor Engin Akkaya. He was a postdoctoral fellow in the laboratory of Sir Fraser Stoddart at NU, and is presently an assistant professor at the Korea Advanced Institute of Science and Technology.

J. Fraser Stoddart received all (B.Sc., Ph.D., D.Sc.) of his degrees from the University of Edinburgh, U.K. Presently, he holds a Board of Trustees Professorship in the Department of Chemistry at NU. His research has opened up a new materials world of mechanically interlocked molecules and, in doing so, has produced a blueprint for the subsequent growth of functional molecular nanotechnology and the fabrication of functional integrated systems.

FOOTNOTES

*Corresponding author. Fax: (+1)-847-491-1009. Tel: (+1)-847-491-3793. E-mail: stoddart@northwestern.edu.
The authors declare no competing financial interest.

REFERENCES

1 Gai, F.; Hasson, K. C.; McDonald, J. C.; Anfinrud, P. A. Chemical Dynamics in Proteins: The Photoisomerization of Retinal in Bacteriorhodopsin. *Science* **1998**, *279*, 1886–1891.

2 Coskun, A.; Banaszak, M.; Astumian, R. D.; Stoddart, J. F.; Grzybowski, B. A. Great Expectations: Can Artificial Molecular Machines Deliver on Their Promise? *Chem. Soc. Rev.* **2012**, *41*, 19–30.

3 Astumian, R. D. Thermodynamics and Kinetics of a Brownian Motor. *Science* **1997**, *276*, 917–922.

4 Kay, E. R.; Leigh, D. A.; Zerbetto, F. Synthetic Molecular Motors and Mechanical Machines. *Angew. Chem., Int. Ed.* **2007**, *46*, 72–191.

5 Michl, J.; Sykes, E. C. H. Molecular Rotors and Motors: Recent Advances and Future Challenges. *ACS Nano* **2009**, *3*, 1042–1048.

6 Liu, Y.; Flood, A. H.; Bonvallet, P. A.; Vignon, S. A.; Northrop, B. H.; Tseng, H.-R.; Jeppesen, J. O.; Huang, T. J.; Brough, B.; Baller, M.; Magonov, S.; Solares, S. D.; Goddard, W. A.; Ho, C.-M.; Stoddart, J. F. Linear Artificial Molecular Muscles. *J. Am. Chem. Soc.* **2005**, *127*, 9745–9759.

7 Eelkema, R.; Pollard, M. M.; Vicario, J.; Katsonis, N.; Ramon, B. S.; Bastiaansen, C. W. M.; Broer, D. J.; Feringa, B. L. Molecular Machines: Nanomotor Rotates Microscale Objects. *Nature* **2006**, *440*, 163.

8 Yamada, M.; Kondo, M.; Mamiya, J.; Yu, Y.; Kinoshita, M.; Barrett, C. J.; Ikeda, T. Photomobile Polymer Materials: Towards Light-Driven Plastic Motors. *Angew. Chem., Int. Ed.* **2008**, *47*, 4986–4988.

9 Stoddart, J. F. The Chemistry of the Mechanical Bond. *Chem. Soc. Rev.* **2009**, *38*, 1802–1820.

10 Juluri, B. K.; Kumar, A. S.; Liu, Y.; Ye, T.; Yang, Y.-W.; Flood, A. H.; Fang, L.; Stoddart, J. F.; Weiss, P. S.; Huang, T. J. A Mechanical Actuator Driven Electrochemically by Artificial Molecular Muscles. *ACS Nano* **2009**, *3*, 291–300.

11 Fang, L.; Hmadeh, M.; Wu, J.; Olson, M. A.; Spruell, J. M.; Trabolsi, A.; Yang, Y.-W.; Elhabiri, M.; Albrecht-Gary, A.-M.; Stoddart, J. F. Acid–Base Actuation of [*c*2]Daisy Chains. *J. Am. Chem. Soc.* **2009**, *131*, 7126–7134.

12 Ambrogio, M. W.; Thomas, C. R.; Zhao, Y.-L.; Zink, J. I.; Stoddart, J. F. Mechanized Silica Nanoparticles: A New Frontier in Theranostic Nanomedicine. *Acc. Chem. Res.* **2011**, *44*, 903–913.

13 Coskun, A.; Spruell, J. M.; Barin, G.; Dichtel, W. R.; Flood, A. H.; Botros, Y. Y.; Stoddart, J. F. High Hopes: Can Molecular Electronics Realise Its Potential? *Chem. Soc. Rev.* **2012**, *41*, 4827–4859.

14 Fahrenbach, A. C.; Bruns, C. J.; Cao, D.; Stoddart, J. F. Ground-State Thermodynamics of Bistable Redox-Active Donor–Acceptor Mechanically Interlocked Molecules. *Acc. Chem. Res.* **2012**, *45*, 1581–1592.

15 Collier, C. P.; Mattersteig, G.; Wong, E. W.; Luo, Y.; Beverly, K.; Sampaio, J.; Raymo, F. M.; Stoddart, J. F.; Heath, J. R. A [2]Catenane-Based Solid State Electronically Reconfigurable Switch. *Science* **2000**, *289*, 1172–1175.

16 Sue, C.-H.; Basu, S.; Fahrenbach, A. C.; Shveyd, A. K.; Dey, S. K.; Botros, Y. Y.; Stoddart, J. F. Enabling Tetracationic Cyclophane Production by Trading Templates. *Chem. Sci.* **2010**, *1*, 119–125.

17 Fahrenbach, A. C.; Barnes, J. C.; Li, H.; Benítez, D.; Basuray, A. N.; Fang, L.; Sue, C.-H.; Barin, G.; Dey, S. K.; Goddard, W. A.; Stoddart, J. F. Measurement of the Ground-State Distributions in Bistable Mechanically Interlocked Molecules Using Slow Scan Rate Cyclic Voltammetry. *Proc. Natl. Acad. Sci. U.S.A.* **2011**, *108*, 20416–20421.

18 Fahrenbach, A. C.; Zhu, Z.; Cao, D.; Liu, W.-G.; Li, H.; Dey, S. K.; Basu, S.; Trabolsi, A.; Botros, Y. Y.; Goddard, W. A.; Stoddart, J. F. Radically Enhanced Molecular Switches. *J. Am. Chem. Soc.* **2012**, *134*, 16275–16288.

19 Flood, A. H.; Peters, A. J.; Vignon, S. A.; Steuerman, D. W.; Tseng, H.-R.; Kang, S.; Heath, J. R.; Stoddart, J. F. The Role of Physical Environment on Molecular Electromechanical Switching. *Chem.—Eur. J.* **2004**, *10*, 6558–6564.

20 Ashton, P. R.; Boyd, S. E.; Brindle, A.; Langford, S. J.; Menzer, S.; Peréz-García, L.; Preece, J. A.; Raymo, F. M.; Spencer, N.; Stoddart, J. F.; White, A. J. P.; Williams, D. J. Diazapyrenium-Containing Catenanes and Rotaxanes. *New J. Chem.* **1999**, *23*, 587–602.

21 Flood, A. H.; Stoddart, J. F.; Steuerman, D. W.; Heath, J. R. Whence Molecular Electronics? *Science* **2004**, *306*, 2055–2056.

22 Tseng, H.-R.; Wu, D.; Fang, N. X.; Zhang, X.; Stoddart, J. F. The Metastability of an Electrochemically Controlled Nanoscale Machine on Gold Surfaces. *ChemPhysChem* **2004**, *5*, 111–116.

23 Hansen, S. W.; Stein, P. C.; Sørensen, A.; Share, A. I.; Witlicki, E. H.; Kongsted, J.; Flood, A. H.; Jeppesen, J. O. Quantification of the π–π Interactions That Govern Tertiary Structure in Donor-Acceptor [2]Pseudorotaxanes. *J. Am. Chem. Soc.* **2012**, *134*, 3857–3863.

24 Spruell, J. M.; Paxton, W. F.; Olsen, J.-C.; Benítez, D.; Tkatchouk, E.; Stern, C. L.; Trabolsi, A.; Friedman, D. C.; Goddard, W. A.; Stoddart, J. F. A Push-Button Molecular Switch. *J. Am. Chem. Soc.* **2009**, *131*, 11571–11580.

25 Asakawa, M.; Ashton, P. R.; Balzani, V.; Credi, A.; Hamers, C.; Mattersteig, G.; Montalti, M.; Shipway, A. N.; Spencer, N.; Stoddart, J. F.; Tolley, M. S.; Venturi, M.; White, A. J. P.; Williams, D. J. A Chemically and Electrochemically Switchable [2]Catenane Incorporating a Tetrathiafulvalene Unit. *Angew. Chem., Int. Ed.* **1998**, *37*, 333–337.

26 Coskun, A.; Saha, S.; Aprahamian, I.; Stoddart, J. F. A Reverse Donor-Acceptor Bistable [2]Catenane. *Org. Lett.* **2008**, *10*, 3187–3190.

27 Fang, L.; Wang, C.; Fahrenbach, A. C.; Trabolsi, A.; Botros, Y. Y.; Stoddart, J. F. Dual Stimulus Switching of a [2]Catenane in Water. *Angew. Chem., Int. Ed.* **2011**, *50*, 1805–1809.

28 Wang, C.; Cao, D.; Fahrenbach, A. C.; Fang, L.; Olson, M. A.; Friedman, D. C.; Basu, S.; Dey, S. K.; Botros, Y. Y.; Stoddart, J. F. Solvent-Dependent Ground-State Distributions in a Donor-Acceptor Redox-Active Bistable [2]Catenane. *J. Phys. Org. Chem.* **2012**, *25*, 544–552.

29 Jeppesen, J. O.; Nielsen, K. A.; Perkins, J.; Vignon, S. A.; Di Fabio, A.; Ballardini, R.; Gandolfi, M. T.; Venturi, M.; Balzani, V.; Becher, J.; Stoddart, J. F. Amphiphilic Bistable Rotaxanes. *Chem.—Eur. J.* **2003**, *9*, 2982–3007.

30 Jeppesen, J. O.; Nygaard, S.; Vignon, S. A.; Stoddart, J. F. Honing up a Genre of Amphiphilic Bistable [2]Rotaxanes for Device Settings. *Eur. J. Org. Chem.* **2005**, 196–220.

31 Choi, J. W.; Flood, A. H.; Steuerman, D. W.; Nygaard, S.; Braunschweig, A. B.; Moonen, N. N. P.; Laursen, B. W.; Luo, Y.; Delonno, E.; Peters, A. J.; Jeppesen, J. O.; Xu, K.; Stoddart, J. F.; Heath, J. R. Ground-State Equilibrium Thermodynamics and Switching Kinetics of Bistable [2]Rotaxanes Switched in Solution, Polymer Gels, and Molecular Electronic Devices. *Chem.—Eur. J.* **2006**, *12*, 261–279.

32 Trabolsi, A.; Fahrenbach, A. C.; Dey, S. K.; Share, A. I.; Friedman, D. C.; Basu, S.; Gasa, T. B.; Khashab, N. M.; Saha, S.; Aprahamian, I.; Khatib, H. A.; Flood, A. H.; Stoddart, J. F. A Tristable [2]Pseudo[2]Rotaxane. *Chem. Commun.* **2010**, *46*, 871–873.

33 Dey, S. K.; Coskun, A.; Fahrenbach, A. C.; Barin, G.; Basuray, A. N.; Trabolsi, A.; Botros, Y. Y.; Stoddart, J. F. A Redox-Active Reverse Donor-Acceptor Bistable [2]Rotaxane. *Chem. Sci.* **2011**, *2*, 1046–1053.

34 Kang, S.; Vignon, S. A.; Tseng, H.-R.; Stoddart, J. F. Molecular Shuttles Based on Tetrathiafulvalene Units and 1,5-Dioxynaphthalene Ring Systems. *Chem.—Eur. J.* **2004**, *10*, 2555–2564.

35 Anelli, P.-L.; Spencer, N.; Stoddart, J. F. A Molecular Shuttle. *J. Am. Chem. Soc.* **1991**, *113*, 5131–5133.

36 Ashton, P. R.; Ballardini, R.; Balzani, V.; Bĕlohradský, M.; Gandolfi, M. T.; Philp, D.; Prodi, L.; Raymo, F. M.; Reddington, M. V.; Spencer, N.; Stoddart, J. F.; Venturi, M.; Williams, D. J. Self-Assembly, Spectroscopic, and Electrochemical Properties of [*n*]Rotaxanes. *J. Am. Chem. Soc.* **1996**, *118*, 4931–4951.

37 Anelli, P.-L.; Asakawa, M.; Ashton, P. R.; Bissell, R. A.; Clavier, G.; Górski, R.; Kaifer, A. E.; Langford, S. J.; Mattersteig, G.; Menzer, S.; Philp, D.; Slawin, A. M. Z.; Spencer, N.; Stoddart, J. F.; Tolley, M. S.; Williams, D. J. Toward Controllable Molecular Shuttles. *Chem.—Eur. J.* **1997**, *3*, 1113–1135.

38 Ashton, P. R.; Boyd, S. E.; Brindle, A.; Langford, S. J.; Menzer, S.; Pérez-García, L.; Preece, J. A.; Raymo, F. M.; Spencer, N.; Stoddart, J. F.; White, A. J. P.; Williams, D. J. Diazapyrenium-Containing Catenanes and Rotaxanes. *New J. Chem.* **1999**, *23*, 587–602.

39 Bĕlohradský, M.; Elizarov, A. M.; Stoddart, J. F. Speed-Controlled Molecular Shuttles. *Collect. Czech. Chem. Commun.* **2002**, *67*, 1719–1728.

40 Iijima, T.; Vignon, S. A.; Tseng, H.-R.; Jarrosson, T.; Sanders, J. K. M.; Marchioni, F.; Venturi, M.; Apostoli, E.; Balzani, V.; Stoddart, J. F. Controllable Donor-Acceptor Neutral [2]Rotaxanes. *Chem.—Eur. J.* **2004**, *10*, 6375–6392.

41 Braunschweig, A. B.; Dichtel, W. R.; Miljanić, O. Š.; Olson, M. A.; Spruell, J. M.; Khan, S. I.; Heath, J. R.; Stoddart, J. F. Modular Synthesis and Dynamics of a Variety of Donor-Acceptor Interlocked Compounds Prepared by Click Chemistry. *Chem.—Asian J.* **2007**, *2*, 634–647.

42 Yoon, I.; Benítez, D.; Zhao, Y.-L.; Miljanić, O. Š.; Kim, S.-Y.; Tkatchouk, E.; Leung, K. C.-F.; Khan, S. I.; Goddard, W. A.; Stoddart, J. F. Functionally Rigid and Degenerate Molecular Shuttles. *Chem.—Eur. J.* **2009**, *15*, 1115–1122.

43 Coskun, A.; Friedman, D. C.; Li, H.; Patel, K.; Khatib, H. A.; Stoddart, J. F. A Light-Gated STOP-GO Molecular Shuttle. *J. Am. Chem. Soc.* **2009**, *131*, 2493–2495.

44 Li, H.; Zhu, Z.; Fahrenbach, A. C.; Savoie, B. M.; Ke, C.; Barnes, J. C.; Lei, J.; Zhao, Y.-L.; Lilley, L. M.; Marks, T. J.; Ratner, M. A.; Stoddart, J. F. Mechanical Bond-Induced Radical Stabilization. *J. Am. Chem. Soc.* **2013**, *135*, 456–467.

45 Avellini, T.; Li, H.; Coskun, A.; Barin, G.; Trabolsi, A.; Basuray, A. N.; Dey, S. K.; Credi, A.; Silvi, S.; Stoddart, J. F.; Venturi, M. Photoinduced Memory Effect in a Redox Controllable Bistable Mechanical Molecular Switch. *Angew. Chem., Int. Ed.* **2012**, *51*, 1611–1615.

46 Li, H.; Zhao, Y.-L.; Fahrenbach, A. C.; Kim, S.-Y.; Paxton, W. F.; Stoddart, J. F. Degenerate [2]Rotaxanes with Electrostatic Barriers. *Org. Biomol. Chem.* **2011**, *9*, 2240–2250.

47 Hmadeh, M.; Fahrenbach, A. C.; Basu, S.; Trabolsi, A.; Benítez, D.; Li, H.; Albrecht-Gary, A.-M.; Elhabiri, M.; Stoddart, J. F. Electrostatic Barriers in Rotaxanes and Pseudorotaxanes. *Chem.—Eur. J.* **2011**, *17*, 6076–6087.

48 Leigh, D. A.; Wong, J. K. Y.; Dehez, F.; Zerbetto, F. Unidirectional Rotation in a Mechanically Interlocked Molecular Rotor. *Nature* **2003**, *424*, 174–179.